International Journal of Applied Pharmaceutics

ISSN- 0975-7058 Vol 17, Issue 4, 2025

Original Article

ABIRATERONE ACETATE LOADED SODIUM ALGINATE NANOPARTICLES FOR IMPROVING AQUEOUS SOLUBILITY AND DISSOLUTION OF ABIRATERONE ACETATE: PREPARATION AND FORMULATION OPTIMIZATION BY CENTRAL COMPOSITE DESIGN, CHARACTERIZATION

NALLAMUTHU M., UMADEVI S.*

Department of Pharmaceutics, School of Pharmaceutical Sciences, Vels Institute of Science, Technology and Advanced Studies (VISTAS), Pallavaram, Chennai-600117, Tamil Nadu, India

*Corresponding author: Umadevi S.; ***Email: umadevi.sps@vistas.ac.in**

Received: 12 Feb 2025, Revised and Accepted: 23 Apr 2025

ABSTRACT

Objective: Abiraterone acetate is poorly soluble in water and is not effectively absorbed from the gastrointestinal tract**.** The oral bioavailability of abiraterone acetate in humans is predicted to be less than 10% due to these characteristics. The target of the present work was to construct Abiraterone Acetate Loaded Sodium Alginate Nanoparticles (ASNPs) to improve the abiraterone acetate aqueous solubility and dissolution.

Methods: The ASNPs were constructed by using the solvent desolvation method. For ASNPs optimization, the Central Composite Design (CCD) was selected. Particle size and Drug Entrapment Efficiency (DEE) were employed as responses to optimize the independent variable composition using CCD.

Results: According to CCD, 13 formulations were developed. The particle size of 219.5±0.92 nm and DEE of 89.21±0.54% originated from the optimal batch based on the desirability function (0.978). Optimized ASNPs were found with a zeta potential of-46.9±0.65 mV, and *in vitro* drug release of 95.43±0.87%. Optimized ASNPs demonstrated a 28.4-fold increase in the solubility in water compared to pure abiraterone acetate. The *in vitro* drug release evaluation suggests that optimized ASNPs exhibit improved dissolution and sustained drug release compared to the commercial product.

Conclusion: This study concludes that optimized ASNPs overcome the aqueous solubility and dissolution challenges of abiraterone acetate and possess most of the ideal properties required for an oral sustained-release dosage form. This can reduce the dosage, administration time, and systemic toxicity, and improve oral bioavailability compared to the commercial product.

Keywords: Sodium alginate, Abiraterone acetate, Nanoparticles, Central composite design, Aqueous solubility, Dissolution, Oral bioavailability

DOI: https://dx.doi.org/10.22159/ijap.2025v17i4.53942 Journal homepage: https://innovareacademics.in/journals/index.php/ijap

INTRODUCTION

Generating novel chemical entities is difficult due to their poor water solubility. The majority of novel pharmaceutical compounds exhibit unfavorable physicochemical features. Numerous investigations have identified poorly soluble drugs; the majority of compounds belong to categories II or IV of the Biopharmaceutical Classification System (BCS) [1, 2]. These medications dissolve slowly, therefore restricting effective oral absorption and bioavailability. For efficient oral administration and bioavailability development, it will be essential to boost the dissolution rate of weakly water-soluble compounds [3, 4]. In recent times, an extensive number of formulation strategies have been used to improve the oral bioavailability of poorly soluble medicines. Oral bioavailability has been investigated through various traditional approaches, including complexation, co-solvency, salt production, and permeation enhancers. However, the efficiency of each of these kinds of medication delivery systems is restricted [5, 6].

Nanoparticle-based drug delivery systems are a newly established, quickly emerging technology that involves nanoscale substances employed in medical diagnostics as well as to administer medicinal products at particular target areas in a controlled manner [7, 8]. Polymeric nanoparticles offer promising options for the oral delivery of weakly water-soluble drugs because of their superior surface-active properties, enhanced water solubility, stability, nontoxic nature, and superior biocompatibility, which render them efficient carriers to navigate around therapeutic limitations [9, 10]. In the domain of biomedicine, sodium alginate-based nanoparticles have drawn a lot of research attention since they have the possibility of applications in the engineering of tissues, chemotherapy for cancer, and drug and gene delivery. An outstanding instance is the targeted management of cancer chemotherapy drugs using customized nanoparticles functionalized with biodegradable sodium alginate, which exhibited elevated aqueous solubility, controlling the drug release, drug safety, oral bioavailability, and greater drug accumulation and retention time in malignant cells [11-13].

Carcinoma of the prostate is the second-greatest cause of cancer-related mortality in men [14]. Abiraterone acetate, which was approved by the FDA in 2011, is usually prescribed in combination with prednisone for the treatment of patients with prostate carcinomas [15]. After oral consumption, abiraterone acetate hydrolyzes to generate the active abiraterone. The CYP17A1 microsomal enzymes, which are involved in several stages of the androgen synthesis process, are specifically and significantly inhibited by abiraterone. The medication appears to be extremely beneficial in extending the lives of those suffering from prostate cancer [16]. Abiraterone acetate is marketed under the Zytiga® brand. Zytiga® has demonstrated clinical and commercial success; oral administration of abiraterone acetate is extremely challenging [17]. Abiraterone acetate is classified as the fourth category of BCS. The substances are poorly soluble in water and are not effectively absorbed from the gastrointestinal tract. The oral bioavailability of abiraterone acetate in humans is predicted to be less than 10% due to these characteristics; hence, a substantial daily dosage of 1000 mg (a total of four 250 mg tablets once a day) is required to reach therapeutic blood levels, which elevates the probability of forgetting doses [18]. Recent work has shown that nanoparticles can greatly enhance the solubility of drugs and their delivery to targets, reducing the systemic side effects caused by poorly water-soluble drugs [19]. Since abiraterone acetate has poor aqueous solubility, its bioavailability is limited and therefore its therapeutic effect is diminished. Increasing its solubility using nanoparticle-based drug delivery systems may lead to greater absorption and better clinical results in prostate cancer patients. Therefore, abiraterone acetate is essential to develop a polymeric nanoparticulate drug delivery system that enhances aqueous solubility, and dissolution, sustaining the drug release, oral bioavailability, and reducing dosing frequency.

A critical step in the design of a polymeric nanoparticle is formulation optimization. Various methods and strategies can be implemented to create input variable composition in nanoparticle development. The traditional method, which is most frequently used, involves modifying one independent variable or component while maintaining the remaining variables unchanged to observe how composition or process variables affect quality attributes. Nevertheless, this method necessitates a lot of research studies, and it proves difficult to fig. out how input components interact with output. It's also possible to misunderstand the experiment results [20]. Using the design of experiment techniques, like Central Composite Design (CCD), throughout the design and development phase could help solve this issue by concurrently identifying the interconnected impact of many factors that affect the outputs' quality. Furthermore, CCD proved successfully implemented in several research investigations for formulation creation and optimization since the data derived from CCD proved reliability and precision in predictions [21].

This study uses the biodegradable sodium alginate polymer to construct polymeric nanoparticles of abiraterone acetate to resolve the biopharmaceutical challenges of abiraterone acetate. So, the study aimed to employ a CCD to optimize the formulation of Abiraterone Acetate Loaded Sodium Alginate Nanoparticles (ASNPs) by investigating the effects of two independent variables (sodium alginate and stirring speed) on the particle size and Drug Entrapment Efficiency (DEE) as dependent variables. It was also anticipated that the use of CCD in this investigation would reduce experimental time and improve comprehension of the process and final output. It uses risk-based concepts and research to recognize the critical factors and optimize them. Subsequently, optimized ASNPs were investigated for particle size, zeta potential, DEE, surface morphology, X-Ray Diffraction (XRD) studies**,** Fourier Transform Infrared Spectroscopy (FTIR), and *in vitro* drug release was carried out. The optimized ASNPs were subjected to accelerated stability testing for six months.

MATERIALS AND METHODS

Materials

Sun Pharmaceutical Industries Ltd in India provided a gift sample of abiraterone acetate. Sodium alginate and Sodium tripolyphosphate were purchased from Nice Chemical Private Ltd in Kerala. Other chemicals are used as analytical grades.

Methods

Analytical method for estimating abiraterone acetate

In this study, abiraterone acetate was quantified using an Ultra Violet (UV) spectrophotometric method for characterization tests. In the ethanol stock solution, the absorbance has been determined at 252 nm. The amount of abiraterone acetate in pH 7.4 phosphate buffer solution was determined by diluting the stock solution to obtain a series of dilutions: 5, 10, 15, 20, and 25 µg/ml of solution. The absorbance of the solution was then measured at 252 nm [22].

Preparation of nanoparticles

The solvent desolvation technique was used to produce ASNPs [23-25]. Sodium alginate (81.8 mg) was dissolved in 10 ml of distilled water. Abiraterone acetate (250 mg) dissolved in 10 ml of ethanol. Combine the abiraterone acetate and sodium alginate solution, and the pH level was adjusted to four. Under continuous stirring (700 rpm), 10 ml of ethanol was added dropwise to the abiraterone acetate-sodium alginate solution. The endpoint was determined by the appearance of turbidity in the solution. 2% sodium tripolyphosphate was then added. For 12 h, the stirring (at 700 rpm) was maintained to allow the nanoparticles to cross-link. Centrifuging the generated solution for 30 min, discarding the supernatant solution, and collecting the precipitate, which was freeze-dried [Freezing temperature and time: −80 °C: 4 h**,** sublimation: shelf temperature (−50 °C), chamber pressure (50–100m Torr), drying time (24 h), secondary drying: shelf temperature (+25 °C), chamber pressure (10–50 m Torr), drying time (6 h)] and stored in the refrigerator for subsequent evaluation investigations.

Determination of quality target product profile (QTPP)

QTPP is a prospective summary of the key characteristics that a drug product or nanoparticle formulation should possess to ensure desired quality, safety, and efficacy. It serves as the foundation for product development and guides the identification of Critical Quality Attributes (CQAs) [26].

Experimental design

The ASNPs were optimized using design-expert software, trial version (13), utilizing a 13-run, 2-factor, 2-level CCD. The sodium alginate concentration (A) and stirring speed (B) (table 1) were chosen as the independent factors based on the preliminary study, and their impacts were investigated on the dependent variables of particle size and DEE. The response variables were subjected to an ANOVA analysis, which is always necessary for evaluating the applicability and validity of the mathematical models, response surface methodology recommends. Each of the variables was assessed via an F test and the outcomes were processed through multiple regression analyses. If the p-value was less than 0.05, the statistical model was considered significant. The response variable's variance, which is further explained by the process variable, was calculated using the R^2 value.

Table 1: Selection of input variables and their level for the CCD

Variable	Levels	
	Low	High
A-Sodium alginate concentration (mg)	50	100
B-Stirring speed (rpm)	100	700
Response variables	Goal	
Y1-Particle size (nm)	Minimize	
Y2-DEE (%)	Maximize	

Characterization of optimized ASNPs

Drug polymer compatibility studies

The FTIR spectroscopic assessment was executed using a Shimadzu FTIR Spectrophotometer, and investigating the drug-polymer compatibility, the KBR pellet method was used to capture the FTIR spectra of pure abiraterone acetate, sodium alginate, and optimized ASNPs. The spectra were taken at a range of 4000 cm^{-1} to 400 cm^{-1}.

XRD

A powder XRD has examined the diffraction images of the pure abiraterone acetate and optimized ASNPs. Pure abiraterone acetate and optimized ASNPs were inserted in a glass sample holder and measurement conditions were scanned at 30 mA and 40 kV, Scan Range (2θ): 5° to 80°, Target: Cu.

Saturated aqueous solubility study

To determine the aqueous solubility of optimized ASNPs and pure abiraterone acetate, an excess amount of each was added to separate flasks containing 10 ml of distilled water. The flasks were placed in a mechanical shaker for 24 h at 37 °C and 100 rpm. Following 24 h, the dispersions were allowed to reach equilibrium, and the supernatant was separated and filtered (0.45µm membrane), and analyzed using UV spectroscopy at 252 nm [27].

Determination of particle size and zeta potential

Using a Malvern Zeta Sizer, the particle size, and zeta potential of ASNPs were assessed. In short, the ASNPs were diluted 1:100 times with water, and the measurement of particle size, Poly Dispersity Index (PDI), and zeta potential was conducted at 25 °C [28].

Determination of DEE

The 10 mg of ASNPs were mixed with 10 ml of water and then centrifuged for 30 min at 10,000 rpm. The unentrapped abiraterone acetate was extracted from the nanoparticles by collecting the supernatant fraction and diluting it suitably with ethanol. The supernatant fraction was collected and suitably diluted with ethanol and filtered (0.45µm membrane). The amount of unentrapped abiraterone acetate in the nanoparticles was determined by UV spectrometric detection at a wavelength of 252 nm [29]. To calculate the DEE, the following formula was applied,

$$\text{DEE\%} = \frac{(\text{Total amount of drug} - \text{Amount of free drug})}{(\text{Total amount of drug})} \times 100$$

***In vitro* drug release**

The *in vitro* release of abiraterone acetate from produced nanoparticles and commercial product (Zytiga®) has been studied using USP dissolving equipment II (paddles) [30]. The commercial product (Zytiga® tablet) and 250 mg of optimized ASNPs were dispersed in 1 ml phosphate buffer (pH 7.4), filled with a dialysis bag, and both were separately put inside the dissolving tester containing 900 ml of phosphate buffer (pH 7.4). To control sink conditions and temperature, this instrument was fitted in an outside water bath. The testing procedure proceeded with stirring at 100 rpm and 37±0.5ºC. The release medium was collected and replaced with a new buffer solution in a separate dissolving vessel at predefined intervals. After sampling and filtering 10 ml of the dissolving medium using a membrane filter (0.45µm), the concentration of abiraterone acetate in the filtrate was measured using UV spectrophotometry at a wavelength of 252 nm.

Surface morphology

The surface morphology of optimized ASNPs and pure abiraterone acetate has been studied using a Scanning Electron Microscope (SEM). Using an accelerating voltage of 20 kV, photomicrographs were made of the sample at various magnifications using a piece of double-sided sticky tape coated with gold.

Accelerated stability studies

Short-term stability investigations were conducted on ASNPs for six months at accelerated conditions of 40±2 °C/75±5% RH. The glass container storing the optimized ASNPs was kept in a stability chamber. The DEE, *in vitro* drug release, and particle size of ASNPs were assessed every three months [31].

RESULTS AND DISCUSSION

Analytical method for estimating abiraterone acetate

The current analytical technique complied with Beer's rule within the measured concentration range of 5–25µg/ml, which rendered it appropriate for abiraterone acetate quantification in phosphate buffer with a pH of 7.4. The linear regression's R^2 value was discovered to be 0.9981. Y=0.0395x+0.0122 is the calibration curve linear regression equation (fig. 1).

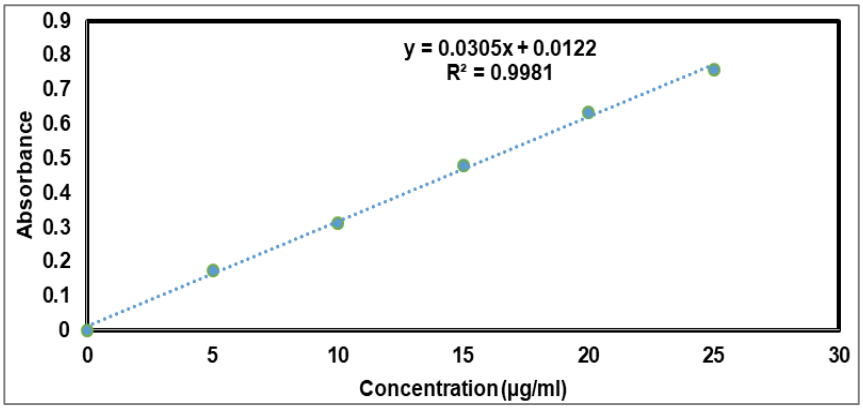

Fig. 1: Calibration graph of abiraterone acetate

Preparation of ASNPs

The desolvation process was used to prepare thirteen batches of ASNPs (table 2). Sodium alginate was chosen in the preparation due to its outstanding biocompatibility, extended storage stability, and expressed capacity to form nanostructures [11-13].

Determination of QTPP

The oral bioavailability and therapeutic effectiveness of medicine are significantly influenced by its solubility [32]. Nanoparticles play an important role in solubility enhancement. Because smaller particles have a greater surface area when exposed to the solvent, it greatly enhances their solubility. An important determinant of nanoparticles' ability to effectively target malignant cells is their size. The optimal particle size is less than 400 nm since this might prolong the nanoparticles' time in the bloodstream and make it possible to target malignant cells specifically through increased permeability and retention [33].

DEE is an important consideration in the design and development of nanoparticle-based drug delivery systems, and assessing the amount of therapeutic agent that was successfully confined within the nanoparticles to the entire quantity of drug used during formulation. High DEE, which ensures that the nanoparticles contain the optimum amount of the active pharmaceutical ingredient, has rendered it potential for drugs to be distributed to the desired location effectively. A high DEE enhances the therapeutic effect by regulating the release of the medicine at the intended location [34, 35].

Therefore, the primary objective of the current study is to reduce the particle size and maximize the entrapment efficiency of abiraterone acetate in sodium alginate nanoparticles, which will enhance the aqueous solubility, and rate of dissolution, sustaining the drug release, therapeutic effect of abiraterone acetate.

Experimental design

The CCD turned out to be the most important and reliable method for screening independent variables in minimal trials in comparison to other designs. To construct ASNPs, the primary impact of an independent variable on dependent variables has to be anticipated. A review of the literature and preliminary investigation contributed to the selection of sodium alginate (A) and stirring speed (B) as the independent variables, while particle size (Y1) and DEE (Y2) were found to be the dependent variables that most affected the development of the nanoparticles. Table 1 displays the independent variables along with their levels, while table 2 displays the response variable observations.

Table 2: Composition of ASNPs by CCD

Run	Factor 1	Factor 2	Response 1	Response 2
	A: Sodium alginate concentration (mg)	B: Stirring speed (rpm)	Particle size (nm)	DEE(%)
1	40	400	353.2±1.03	48.94±0.23
2	100	700	265.9±0.76	85.36±0.45
3	75	200	558.4±1.32	68.25±0.12
4	100	100	957.3±0.98	52.69±0.54
5	50	100	496.2±0.93	45.81±0.37
6	75	400	415.6± 1.45	74.65±0.49
7	75	400	415.6± 1.63	74.65±0.76
8	110	400	698.5± 0.64	80.92±0.12
9	75	400	415.6± 0.45	75.95±0.06
10	50	700	203.2±1.87	68.59±0.05
11	75	400	415.6± 0.04	74.65±0.23
12	75	800	225.8±1.08	84.95±0.05
13	75	400	415.6±0.32	74.65±0.87

Data are expressed in mean±SD (n = 3)

Effect of an independent variable on the particle size of ASNPs

The ASNPs were discovered to have an average particle size ranging from 203.2±1.87 to 957.3±0.98 nm (table 2). The polynomial model revealed that significant effects are caused by input variables such as stirring speed (B) and sodium alginate (A). Particles that are expected and actual appear with values that are closest together (fig. 2). The F-value of 105.6 confirms the statistical significance of the model, supporting the mathematical model's significance developed for the mean particle size of ASNPs. The F-value is large and could only be a consequence of noise with a 0.01% chance. Since P values below 0.05 suggest considerable modeling terms, the quadratic term has a considerable impact on particle size (table 3). The graphs of contour and three-dimensional response surfaces were implemented to clarify further the consequences of the major and interacting effects associated with the input variables on the particle size of ASNPs. Fig. 3 indicates the matching contour plot interaction between A and B on the particle size of ASNPs. The 3D response surface graphs (fig. 4) explain the connection between the input variable [Sodium alginate (A), Stirring speed (B), and the output variables (Particle size)]. The relationship between stirring speed (B) and sodium alginate concentration (A) concerning ASNPs particle size can be observed in the interaction graph (fig. 5).

The consequence of factor levels on particle size can be explained by the following polynomial equation.

$$\text{Particle size} = 413.32+127.20A-226.60B-99.54\,AB+47.84A^2+37.94B^2$$

As a result, the maximum concentration of sodium alginate resulted in smaller ASNPs particle sizes, while increasing the concentration of sodium alginate resulted in larger ASNPs. As the speed of stirring increased, the size of the ASNPs decreased. The particle size of ASNPs can be efficiently reduced by using a maximum concentration of sodium alginate and increasing the stirring speed (fig. 3-5). Table 3 describes the statistical analysis of particle size (ANOVA). Thus, the given model was significant (p value 0.0001).

Table 1: Statistical analysis of particle size (ANOVA)

Parameters	DF	SS	MS	F value	P value	R^2	SD	C. V.%	Adj R^2	Predicted R^2
Particle size										
Model	5	4.86	97380.65	105.6	0.0001	0.9868	30.45	6.78	0.9775	0.9049
Residual	7	6488.66	926.95							

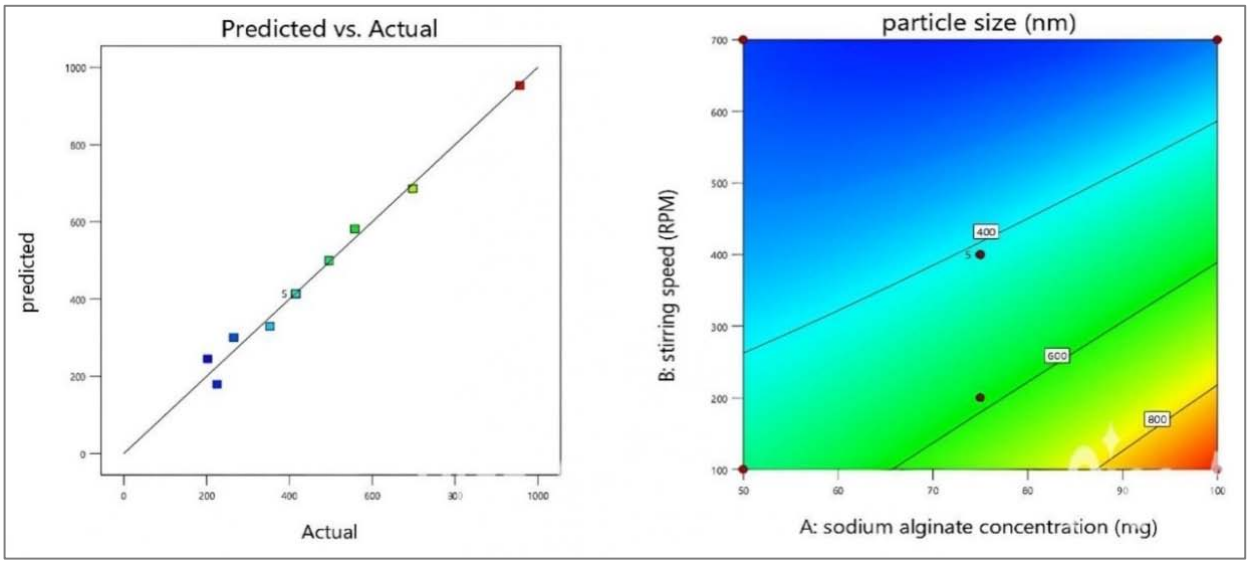

Fig. 2, 3: Predicted v/s actual correlation of particle size, contour plot for sodium alginate concentration and stirring speed against particle size

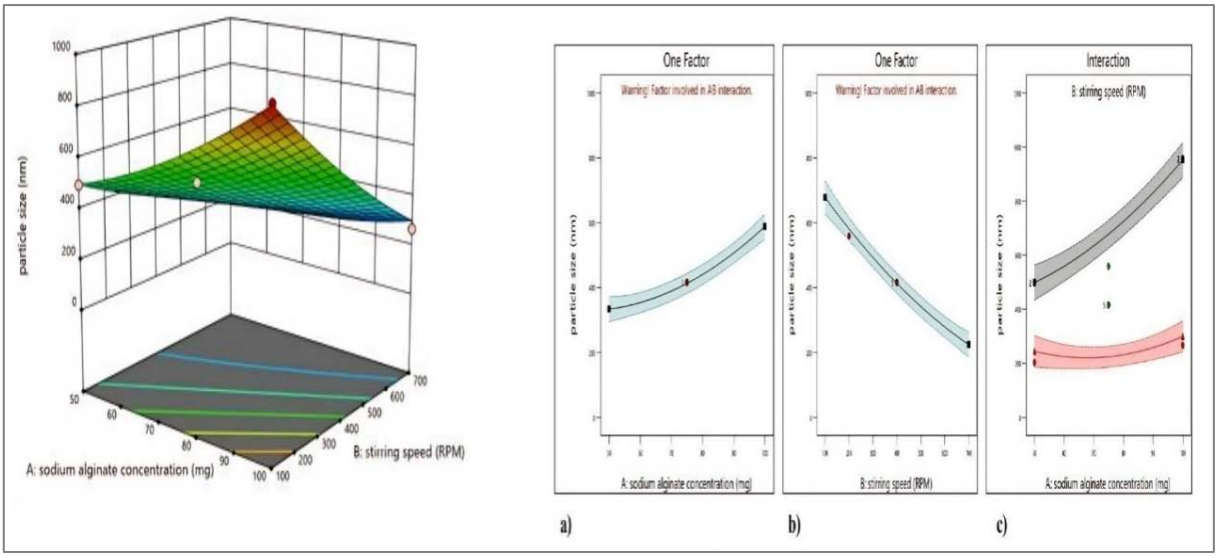

Fig. 4, 5: 3D surface plots sodium alginate concentration and stirring speed against particle size, Interaction graph for sodium alginate concentration (a), stirring speed (b), sodium alginate concentration, and stirring speed (c) on particle size

Effect of an independent variable on DEE

The range of 45.81±0.37% to 85.36±0.45% was determined to represent the entrapment efficiency of abiraterone acetate in ASNPs (table 2). According to the polynomial model, each variable (A, B) has a notable impact. As fig. 6 illustrates that the observed values correspond closely to the expected values. The F-value of 30.73 suggested that the mathematical model created for DEE (Y2) was significant (table 4). The interaction effects of the independent factors on the DEE were further elucidated through contour plots and 3D surface plots. Fig. 7 indicates the matching contour plot interaction between sodium alginate (A) and stirring speed (B) on the DEE. 3D response surface graphs (fig. 8) explain the connection between the input variables [Sodium alginate (A), stirring speed (B)] and the output variables (DEE)]. The relationship between stirring speed (B) and sodium alginate concentration (A) concerning DEE can be observed in the interaction graph (fig. 9). Thereby, the presented model was significant. The consequence of factor levels on particle size can be explained by the following polynomial equation.

$$DEE = 75.59+8.64\ A+13.55\ B+2.476AB-5.95\ A^2-5.55\ B^2$$

Therefore, abiraterone acetate entrapment in the designed nanoparticle increased with increasing sodium alginate concentration (A) and stirring speed (B); conversely, abiraterone acetate entrapment in the designed nanoparticle decreased with decreasing sodium alginate concentration and stirring speed. Increasing the sodium alginate concentration and stirring speed will result in the maximum drug entrapment (fig. 7-9). The statistical analysis of DEE (ANOVA) is described in table 4. Table 4 describes a statistical model that was significant (p value-0.0001) effect.

Table 2: Statistical analysis of DEE

Parameters	DF	SS	MS	F value	P value	R^2	SD	C. V. %	Adj R^2	Predicted R^2
DEE										
Model	5	1945.32	389.06	30.73	0.0001	0.9564	3.56	5.08	0.9253	0.5190
Residual	7	88.62	12.66							

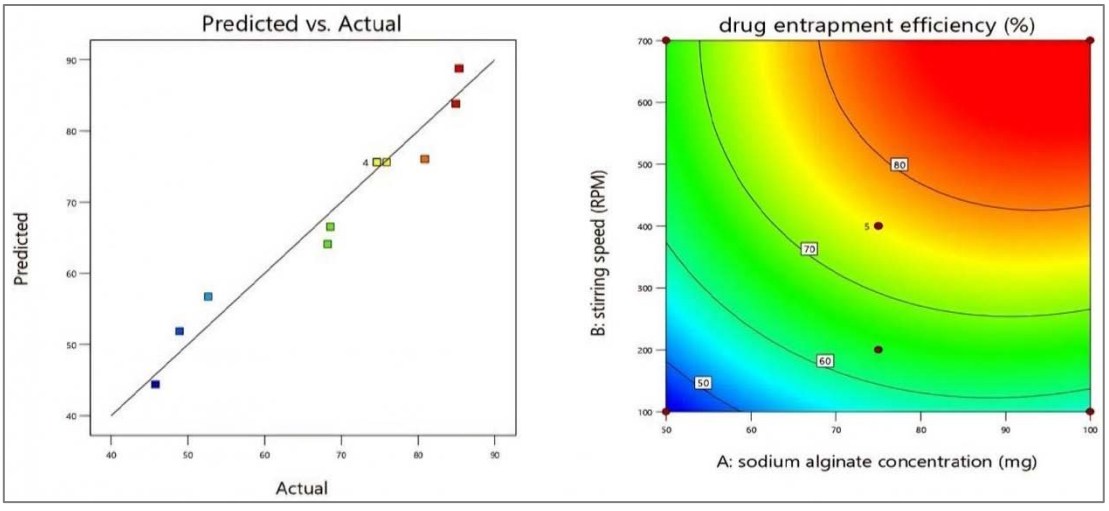

Fig. 6, 7: Predicted v/s actual correlation of DEE, contour plot for sodium alginate concentration and stirring speed against DEE

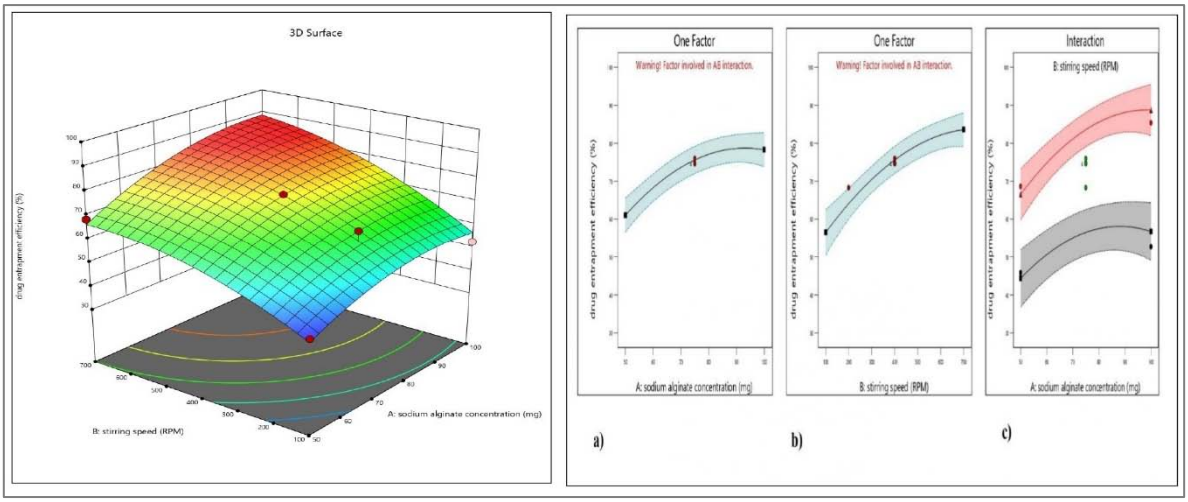

Fig. 8, 9: 3D surface plots sodium alginate concentration and stirring speed against DEE, Interaction graph for sodium alginate concentration (a), stirring speed (b), sodium alginate concentration, and stirring speed on DEE

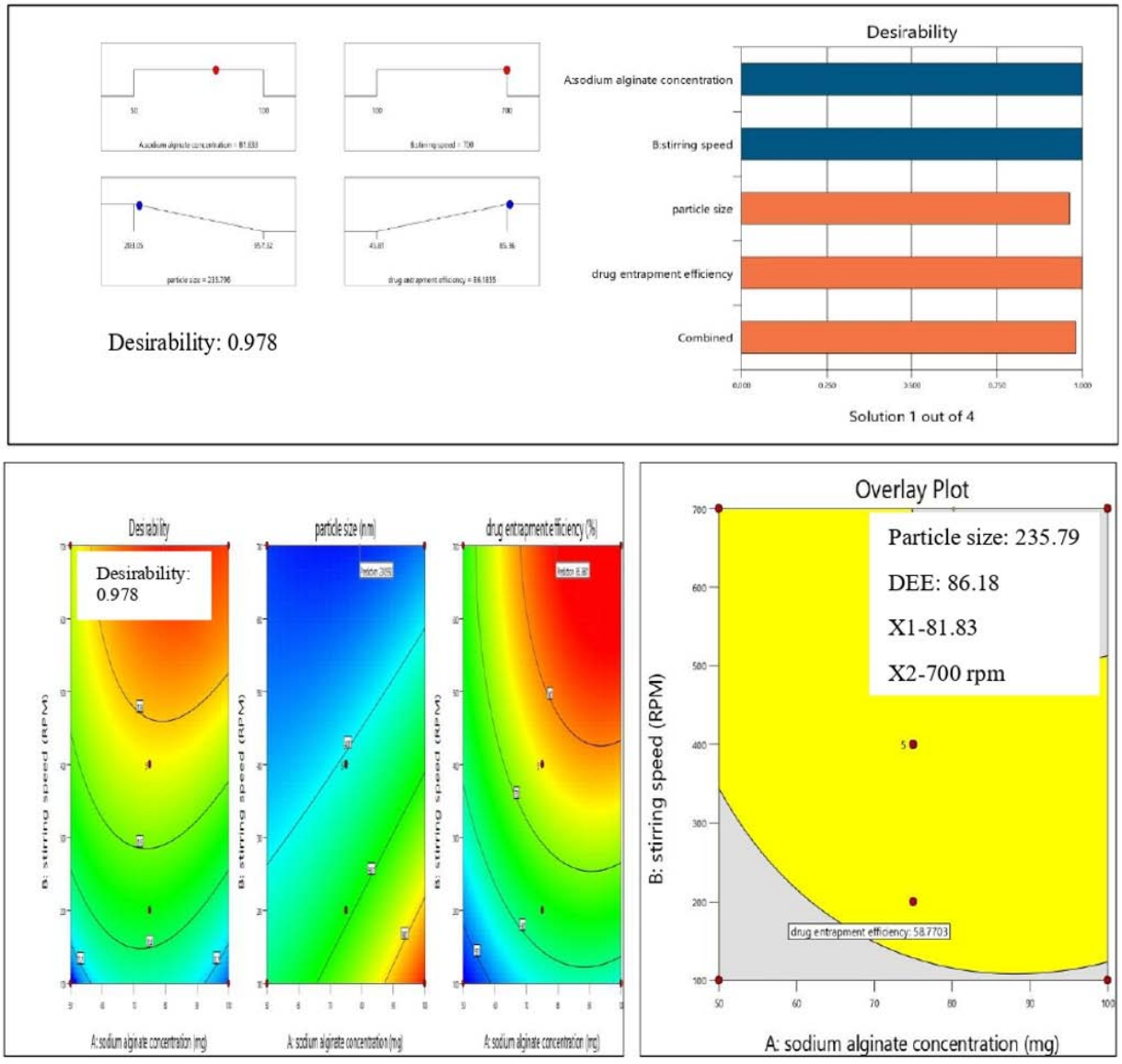

Fig. 10, 11: Desirability graphs-ramp and bar graphs, graphical optimization of ASNPs-a) Contour plot, b) overlay plot

Optimization of ASNPs

The numerical (fig. 10) and graphical optimization (fig. 11) were used to pick the optimized ASNPs formula because it exhibits a high desirability function (0.978) as seen in fig. 10 and fig. 11. The composition of the optimized ASNPs formulation included sodium alginate (81.83 mg), and stirring speed (700 rpm), The formulation demonstrated the expected values for particle size (235.79), and DEE (86.18%) as depicted in fig. 10, 11.

Confirmation of optimized formula for ASNPs

The confirmation findings showed that the observed residual error of particle size and DEE for optimized formulations was less than 10% (table 5). It validates the optimization findings by demonstrating a high degree of agreement between the projected and actual results. The residual error and observed outcomes show that CCD has been successfully utilized to optimize the ASNPs optimal formula and satisfy the predetermined objective listed in table 1.

Table 5: Confirmation results of optimized ASNPs

Optimized ASNPs formula		Responses	Predicted value	Observed value	Residual error
Sodium alginate (mg)	Stirring speed (rpm)				
81.83 mg	700 rpm	Particle size (nm)	235.7	219.5± 0.92	6.8%
		DEE (%)	86.18	89.21± 0.54	3.52%

Evaluation of optimized ASNPs

Drug–polymer compatibility study

The compatibility of the drug and polymer was confirmed using FTIR spectroscopy investigations. The sodium alginate, abiraterone acetate, and optimized ASNPs FTIR spectra were recorded (table 6 and fig. 12). It showed that the characteristic peak of pure abiraterone acetate was not altered by the addition of excipients and after formulated into nanoparticle with no change in functional group and indicating no chemical reaction and interaction between the drug and excipients (fig. 12). The predominant peaks of sodium alginate and abiraterone acetate in the optimized ASNPs spectra indicate that the drug and polymer are compatible.

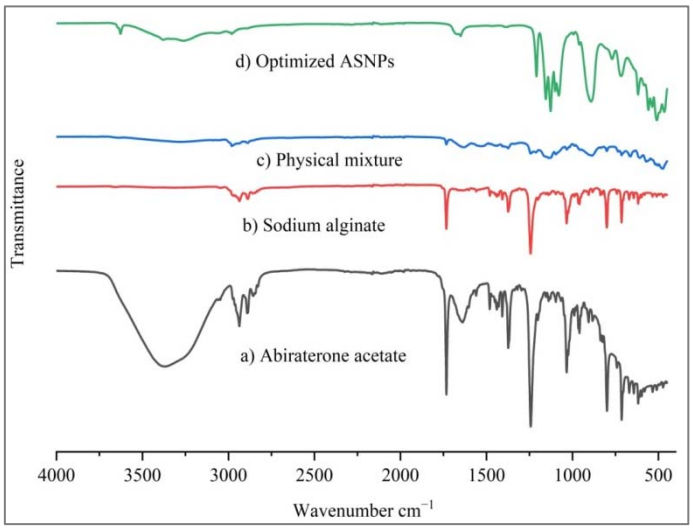

Fig. 12: FTIR spectrum of pure abiraterone acetate (a), Sodium alginate (b), Physical mixture (c), Optimized ASNPs (d)

Table 6: FTIR interpretation of abiraterone acetate, sodium alginate, physical mixture, optimized ASNPs

Functional groups	Pure abiraterone acetate	Sodium Alginate	Physical mixture	Optimized ASNPs
C-H starching	2891.74	-	2891.74	2936.09
	2936.09		2936.09	
Ester	1734.66	-	1735.62	1716.34
				1734.66
C=C stretching	1602.56	-	1600.63	1540.85
	1588.2		1530.24	1507.1
OH stretching	3562.78	3565.74	3637.09	3445.21
C=O stretching	1716.42	1716.34	1710.55	1716.34
Pyridine ring	1485.04	-	1484.42	1485.08

XRD

XRD patterns of pure abiraterone acetate and optimal ASNPs are shown in fig. 13. Variable crystal structures of abiraterone acetate are shown in fig. 13a-b. The pure abiraterone acetate X-ray patterns exhibited distinct peaks at 13.270°, 15.000°, 18.256°, 19.800°, 25.160°, 32.100°, and 64.499° [36]. Such intense and sharp diffraction peaks in fig. 13a revealed the crystalline nature of pure abiraterone acetate. A sharp peak at high intensity also indicates well-ordered packing of the molecules. On the other hand, fig. 13b indicates broader and less intense peaks, which are suggestive of either a partially crystalline or amorphous structure. Due to the loss of the crystalline lattice, the peaks became less intense, and which remained in the amorphous zone was broad. Fig. 13b may represent optimized ASNPs with an amorphized drug that enhances solubility and bioavailability [37].

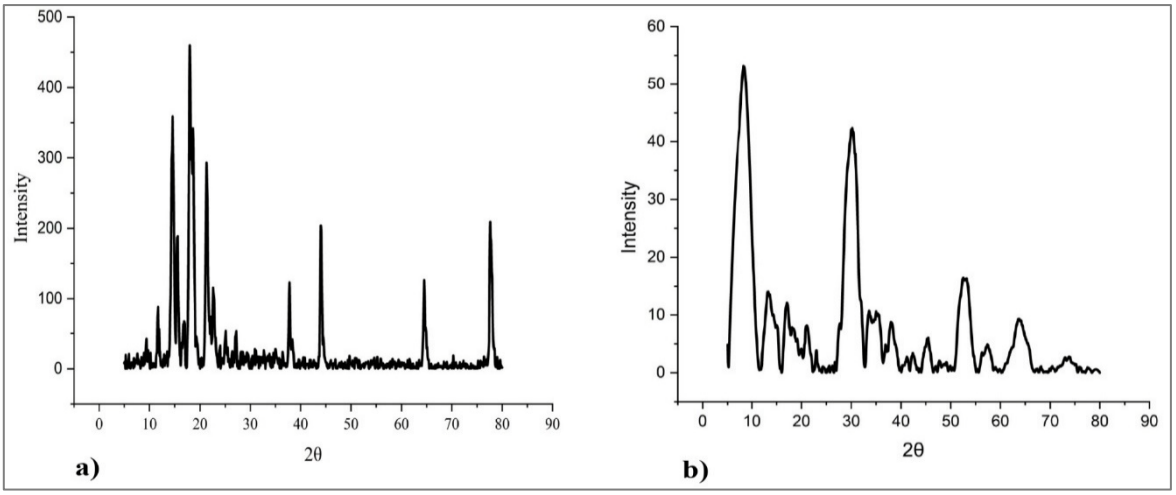

Fig. 13: XRD graphs for pure abiraterone acetate (a), optimized ASNPs (b)

Determination of aqueous saturated solubility study

Comparative evaluation of the aqueous saturated solubility of optimized ASNPs and Pure Abiraterone Acetate reveals that pure abiraterone acetate has a poor aqueous solubility (0.43±0.21µg/ml) after creating optimal ASNPs, its solubility increases to 12.24±1.02µg/ml. Comparative Evaluation of the aqueous saturated solubility of optimized ASNPs reveals that reduced crystalline structure [37], particle size reduction [38], and the masking of the hydrophobic groups of abiraterone acetate by the inclusion of sodium alginate (ASNPs) [39], support the improvement of aqueous solubility. The aqueous solubility in optimized ASNPs showed an increase in solubility by 28.4-fold in distilled water compared to pure abiraterone acetate.

Determination of particle size and zeta potential

The optimized ASNPs had a Z-average particle size of 219.5±0.92 nm (fig. 14). A smaller particle size denotes enhanced water solubility and a quicker rate of dissolution [38]. The effective reduction of particle size is accomplished by the use of a CCD, which optimizes the composition of the input variables.

The optimized ASNPs particle size is smaller than 400 nm since this could increase the nanoparticles' time in the bloodstream and allow for the specific targeting of malignant cells through improved permeability and retention [33]. The optimized ASNPs have a PDI of 0.034. The PDI value indicates that the prepared nanoparticles are highly homogeneous.

The zeta potential of optimized ASNPs is used to determine their surface electric charge. Using an applied electric field to track the movement of nanoparticles, the zeta potential of ASNPs was determined. At 25 °C, the zeta potential was measured with a measuring angle of 90°. The optimized ASNPs zeta potential value was discovered to be-46.9±0.65 mV (fig. 15). The value amply demonstrates the good physical stability of the constructed nanoparticles. The optimized ASNPs have high zeta potential, indicating that the surface was highly negatively charged, which caused the particles to experience intense electrostatic repulsion. The particles are forced to be free by this repulsion, which stops them from aggregating. This distribution can improve aqueous solubility and dissolution by increasing surface area [40].

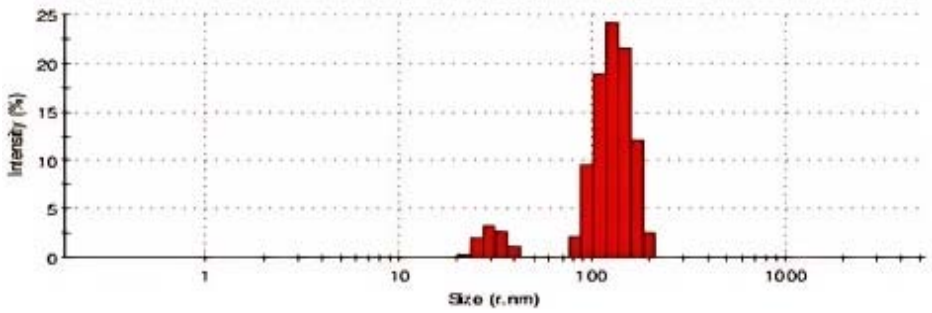

Fig. 14: Particle size of optimized ASNPs

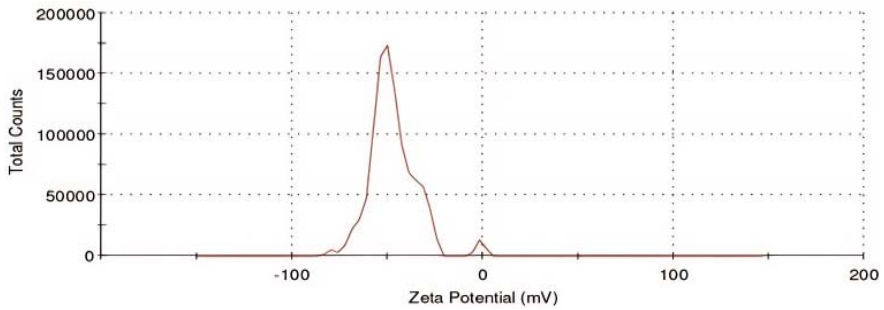

Fig. 15: Zeta potential of optimized ASNPs

Determination of DEE

This work constructs ASNPs with excellent DEE using a CCD. Using a CCD, ASNPs were extensively developed and optimized in the present study. The ASNPs are expected to have greater therapeutic efficacy because of their entrapment efficiency of 89.21±0.54% for abiraterone acetate in produced nanoparticles.

***In vitro* drug release studies**

The commercial product (Zytiga®) and optimized ASNPs were tested for cumulative percentage drug release. Fig. 16 highlights only 60.54±0.67% of the abiraterone acetate is released from commercial product after 12 h in dissolving media, which can be attributed to its poor solubility. According to the *in vitro* release profile of ASNPs, in the first 2 h, almost 60.21±0.67% abiraterone acetate was released from optimized ASNPs, after a burst release, there was a sustained release (95.43±0.87%) for 12 h from optimized ASNPs (fig. 16).

Abiraterone acetate nanosizing [38], the presence of sodium alginate [39], and a decrease in the drug crystallinity [37] in prepared nanoparticles (ASNPs) contribute to the increased aqueous solubility and dissolution of abiraterone acetate. The kinetics of abiraterone acetate release from optimized ASNPs were determined by measuring the R^2 value for distinct kinetic models. The results found that the Korsmeyer-Peppas model exhibited the highest R^2 value. Our findings showed optimized ASNPs in the Korsmeyer-Peppas model showed the highest R^2 and n value of 1.75 in the dissolving medium (table 7). As suggested by the Korsmeyer model, abiraterone acetate can be released from optimized ASNPs through super case 2 transport, abiraterone acetate release process in ASNPs involves substantial matrix swelling and diffusion in the dissolution medium.

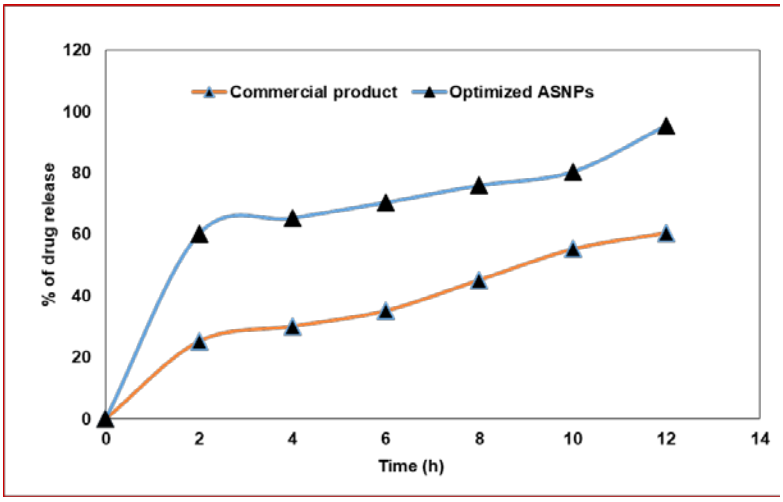

Fig. 16: Dissolution profile of optimized ASNPs and commercial product (Zytiga®), the results were reported (n = 3)

Table 7: Drug release kinetics of optimized ASNPs

Optimized ASNPs	Zero-order	First order	Higuchi model	Korsmeyer-Peppas model
R^2 value	0.7094	0.9320	0.7096	0.9670

Surface morphology

Fig. 17ab exhibits an SEM picture of optimized ASNPs and pure abiraterone acetate. Compared to pure abiraterone acetate, SEM pictures of optimized ASNPs showed a change in surface shape. Pure abiraterone has large crystal shapes (fig. 17a) and optimized ASNPs have smooth edges and rod-like crystal shapes (fig. 17b). Abiraterone acetate was amalgamated in produced nanoparticles (ASNPs) as evidenced by SEM pictures (fig. 17b); this could probably account for the enhancement of aqueous solubility and dissolution.

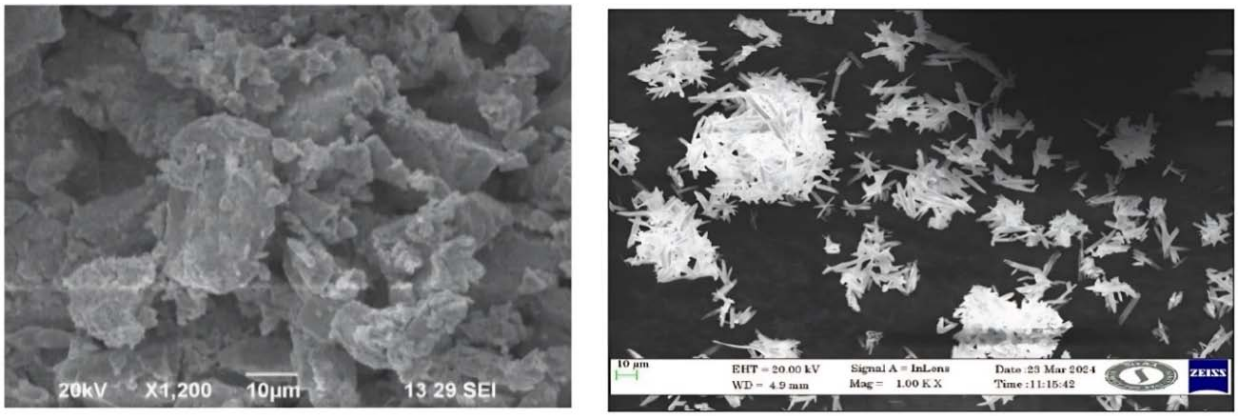

a) b)

Fig. 17: SEM graphs (a) pure abiraterone acetate and (b) optimized ASNPs

Accelerated stability studies

Accelerated stability tests were performed over six months to check the stability of the optimally developed ASNPs. Therefore, zeta potential, particle size, DEE, and in vitro drug release studies systematically assessed during this bid over some defined intervals were presented in table 8. Particle size showed no significant change, suggesting that the nanoparticles were well-dispersed with no aggregation. Stability was also provided by the zeta potential values, which confirmed that the surface charge and therefore the stability did not change. In addition, they showed that no drug leakage occurred or, in other words, that there was no variation of DEE. The *in vitro* drug release profile was found to be consistent with the original formulation, thereby establishing that the optimized ASNPs shall maintain their drug-release property with time. Collectively, those findings confirm the chemical stability of the optimized ASNPs under accelerated stability conditions.

Table 8: Accelerated stability testing of optimized ASNPs

Characterization studies	Storage condition	Before testing	3rd mo	6th mo
Particle size	40±2 °C/75±5% RH	219.5±0.92 nm	219.5±0.23 nm	220.07±0.26 nm
Zeta potential		-46.9±0.65 mV	-46.95±0.74 mV	-47.12 ±0.41 mV
DEE		89.21±0.54%	89.45±0.97%	89.76±0.56%
In vitro drug release		95.43±0.87%	95.96±0.43%	96.05±0.74%

Data are expressed in mean±SD (n = 3)

CONCLUSION

The optimization of the ASNPs was successfully finished to produce nano-sized ASNPs (219.5±0.92 nm). The findings of the studies indicate that the optimized ASNPs from the CCD technique were credible and efficient. The response surface plots generated by this study provided an obvious comprehension of the connection between sodium alginate and stirring speed, which is the main factor in the formulation of ASNPs, along with how it impacts particle size and DEE. Consequently, the optimal input variable composition of ASNPs, as predicted by the CCD, was satisfactory. The analysis of the DEE (89.21±0.54%) revealed that abiraterone acetate was entrapped effectively in optimized ASNPs and therefore, is anticipated to increase its therapeutic efficacy. The optimized ASNPs zeta potential value was discovered to be-46.9±0.65 mV. The value amply demonstrates the good physical stability of the constructed nanoparticles. Optimized ASNPs demonstrated a 28.4-fold increase in the solubility in water compared to pure abiraterone acetate. The *in vitro* drug release evaluation suggests that ASNPs exhibit an improved dissolution (95.43±0.87%) compared to commercial product (Zytiga®). In accelerated stability testing, optimized ASNPs were stable for six months. Optimized ASNPs overcome the aqueous solubility, and dissolution challenges of abiraterone acetate and possess most of the ideal properties required for an oral sustained-release dosage form. Therefore, the studied ASNPs might be useful in the treatment of prostate cancer. This can cause the drug to be distributed at the intended location for a longer period, reducing the dosage, administration time, and systemic toxicity compared to commercial product. However, further studies in pharmacokinetics (*in vivo* tests) are needed to prove clinical efficacy.

ACKNOWLEDGEMENT

The authors are thankful to Vels Institute of Science, Technology and Advanced Studies (VISTAS), Pallavaram, Chennai, India for providing the facility to complete this research. The authors acknowledge Sun Pharmaceutical Industries Ltd for providing a gift sample of abiraterone acetate.

FUNDING

This work was not funded by any organization

AUTHORS CONTRIBUTIONS

Mr. M. Nallamuthu completed the research work and writing part and Dr. S. Umadevi made the correction submission for publication

CONFLICT OF INTERESTS

The authors declare that there is no conflict of interest.

REFERENCES

1. Kawabata Y, Wada K, Nakatani M, Yamada S, Onoue S. Formulation design for poorly water soluble drugs based on biopharmaceutics classification system: basic approaches and practical applications. Int J Pharm. 2011;420(1):1-10. doi: 10.1016/j.ijpharm.2011.08.032, PMID 21884771.
2. Amidon GL, Lennernas H, Shah VP, Crison JR. A theoretical basis for a biopharmaceutic drug classification: the correlation of *in vitro* drug product dissolution and *in vivo* bioavailability. Pharm Res. 1995;12(3):413-20. doi: 10.1023/a:1016212804288, PMID 7617530.
3. Pouton CW. Formulation of poorly water soluble drugs for oral administration: physicochemical and physiological issues and the lipid formulation classification system. Eur J Pharm Sci. 2006;29(3-4):278-87. doi: 10.1016/j.ejps.2006.04.016, PMID 16815001.
4. Mitchell MJ, Billingsley MM, Haley RM, Wechsler ME, Peppas NA, Langer R. Engineering precision nanoparticles for drug delivery. Nat Rev Drug Discov. 2021;20(2):101-24. doi: 10.1038/s41573-020-0090-8, PMID 33277608.
5. Amsa P, Tamizharasi S, Jagadeeswaran M, Sivakumar T. Preparation and solid state characterization of simvastatin nanosuspensions for enhanced solubility and dissolution. Int J Pharm Pharm Sci. 2014;6(10):265-9.
6. Hanum TI, Prasetyo BE, Fadilla W. Formulation and *in vitro* test of ketoprofen nanosuspension using the milling method with polymer variations. Int J App Pharm. 2024;16(6):57-63. doi: 10.22159/ijap.2024v16i6.51843.
7. Hemant KS, Raizaday A, Sivadasu P, Uniyal S, Kumar SH. Cancer nanotechnology: nanoparticulate drug delivery for the treatment of cancer. Int J Pharm Pharm Sci. 2015;3:40-6.
8. Rizvi SA, Saleh AM. Applications of nanoparticle systems in drug delivery technology. Saudi Pharm J. 2018;26(1):64-70. doi: 10.1016/j.jsps.2017.10.012, PMID 29379334.
9. Ensign LM, Cone R, Hanes J. Oral drug delivery with polymeric nanoparticles: the gastrointestinal mucus barriers. Adv Drug Deliv Rev. 2012;64(6):557-70. doi: 10.1016/j.addr.2011.12.009, PMID 22212900.
10. Pridgen EM, Alexis F, Farokhzad OC. Polymeric nanoparticle drug delivery technologies for oral delivery applications. Expert Opin Drug Deliv. 2015;12(9):1459-73. doi: 10.1517/17425247.2015.1018175, PMID 25813361.
11. Ahmad A, Mubarak NM, Jannat FT, Ashfaq T, Santulli C, Rizwan M. A critical review on the synthesis of natural sodium alginate based composite materials: an innovative biological polymer for biomedical delivery applications. Processes. 2021;9(1):137. doi: 10.3390/pr9010137.
12. Jadach B, Swietlik W, Froelich A. Sodium alginate as a pharmaceutical excipient: novel applications of a well known polymer. J Pharm Sci. 2022;111(5):1250-61. doi: 10.1016/j.xphs.2021.12.024, PMID 34986359.
13. Cui Z, Zhang Y, Zhang J, Kong H, Tang X, Pan L. Sodium alginate functionalized nanodiamonds as sustained chemotherapeutic drug release vectors. Carbon. 2016;97:78-86. doi: 10.1016/j.carbon.2015.07.066.

14. Butler EN, Kelly SP, Coupland VH, Rosenberg PS, Cook MB. Fatal prostate cancer incidence trends in the United States and England by race stage and treatment. Br J Cancer. 2020;123(3):487-94. doi: 10.1038/s41416-020-0859-x, PMID 32433602.
15. Fizazi K, Tran N, Fein L, Matsubara N, Rodriguez Antolin A, Alekseev BY. Abiraterone plus prednisone in metastatic castration sensitive prostate cancer. N Engl J Med. 2017;377(4):352-60. doi: 10.1056/NEJMoa1704174, PMID 28578607.
16. Stappaerts J, Geboers S, Snoeys J, Brouwers J, Tack J, Annaert P. Rapid conversion of the ester prodrug abiraterone acetate results in intestinal supersaturation and enhanced absorption of abiraterone: *in vitro* rat in situ and human *in vivo* studies. Eur J Pharm Biopharm. 2015;90:1-7. doi: 10.1016/j.ejpb.2015.01.001, PMID 25592324.
17. US FDA. Clinical pharmacology and biopharmaceutics review(s)-Zytiga®; 2010. Available from: https://www.fda.accessdata.gov/drugsatfdadocs/nda/2011/202379orig1s000clinpharmr.pdf. [Last accessed on 10 Apr 2024].
18. Schultz HB, Meola TR, Thomas N, Prestidge CA. Oral formulation strategies to improve the bioavailability and mitigate the food effect of abiraterone acetate. Int J Pharm. 2020;577:119069. doi: 10.1016/j.ijpharm.2020.119069, PMID 31981706.
19. Liu Y, Liang Y, Yuhong J, Xin P, Han JL, DU Y. Advances in nanotechnology for enhancing the solubility and bioavailability of poorly soluble drugs. Drug Des Dev Ther. 2024 May 1;18:1469-95. doi: 10.2147/DDDT.S447496, PMID 38707615.
20. Rampado R, Peer D. Design of experiments in the optimization of nanoparticle based drug delivery systems. J Control Release. 2023;358:398-419. doi: 10.1016/j.jconrel.2023.05.001, PMID 37164240.
21. Tavares Luiz M, Santos Rosa Viegas J, Palma Abriata J, Viegas F, Testa Moura DE, Carvalho Vicentini F, Lopes Badra Bentley MV. Design of experiments (DoE) to develop and to optimize nanoparticles as drug delivery systems. Eur J Pharm Biopharm. 2021 Aug;165:127-48. doi: 10.1016/j.ejpb.2021.05.011, PMID 33992754.
22. Akbel E. Development validation and greenness assessment of eco-friendly analytical methods for the determination of abiraterone acetate in pure form and pharmaceutical formulations. Separations. 2024;11(10):290. doi: 10.3390/separations11100290.
23. Weber C, Coester C, Kreuter J, Langer K. Desolvation process and surface characterisation of protein nanoparticles. Int J Pharm. 2000 Jan 20;194(1):91-102. doi: 10.1016/s0378-5173(99)00370-1, PMID 10601688.
24. Krishnamoorthy K, Mahalingam M. Selection of a suitable method for the preparation of polymeric nanoparticles: multi-criteria decision making approach. Adv Pharm Bull. 2015;5(1):57-67. doi: 10.5681/apb.2015.008, PMID 25789220.
25. Reis CP, Neufeld RJ, Ribeiro AJ, Veiga F. Nanoencapsulation I. Methods for preparation of drug loaded polymeric nanoparticles. Nanomedicine. 2006;2(1):8-21. doi: 10.1016/j.nano.2005.12.003, PMID 17292111.
26. Martin Moe S, Lim FJ, Wong RL, Sreedhara A, Sundaram J, Sane SU. A new roadmap for biopharmaceutical drug product development: integrating development validation and quality by design. J Pharm Sci. 2011;100(8):3031-43. doi: 10.1002/jps.22545, PMID 21425164.
27. Obinu A, Porcu EP, Piras S, Ibba R, Carta A, Molicotti P. Solid lipid nanoparticles as formulative strategy to increase oral permeation of a molecule active in multidrug resistant tuberculosis management. Pharmaceutics. 2020;12(12):1132. doi: 10.3390/pharmaceutics12121132, PMID 33255304.
28. Ismail R, Sovany T, Gacsi A, Ambrus R, Katona G, Imre N. Synthesis and statistical optimization of poly (lactic-Co-glycolic acid) nanoparticles encapsulating GLP1 analog designed for oral delivery. Pharm Res. 2019;36(7):99. doi: 10.1007/s11095-019-2620-9, PMID 31087188.
29. Salatin S, Barar J, Barzegar Jalali M, Adibkia K, Kiafar F, Jelvehgari M. Development of a nanoprecipitation method for the entrapment of a very water soluble drug into Eudragit RL nanoparticles. Res Pharm Sci. 2017;12(1):1-14. doi: 10.4103/1735-5362.199041, PMID 28255308.
30. Bai G, Armenante PM, Plank RV, Gentzler M, Ford K, Harmon P. Hydrodynamic investigation of USP dissolution test apparatus II. J Pharm Sci. 2007;96(9):2327-49. doi: 10.1002/jps.20818, PMID 17573698.
31. Muthu MS, Feng SS. Pharmaceutical stability aspects of nanomedicines. Nanomedicine (Lond). 2009;4(8):857-60. doi: 10.2217/nnm.09.75, PMID 19958220.
32. Zhuo Y, Zhao YG, Zhang Y. Enhancing drug solubility bioavailability and targeted therapeutic applications through magnetic nanoparticles. Molecules. 2024;29(20):4854. doi: 10.3390/molecules29204854, PMID 39459222.
33. Subhan MA, Yalamarty SS, Filipczak N, Parveen F, Torchilin VP. Recent advances in tumor targeting via EPR effect for cancer treatment. J Pers Med. 2021;11(6):571. doi: 10.3390/jpm11060571, PMID 34207137.
34. Singh R, Lillard JW JR. Nanoparticle based targeted drug delivery. Exp Mol Pathol. 2009 Jun;86(3):215-23. doi: 10.1016/j.yexmp.2008.12.004, PMID 19186176.
35. Kita K, Dittrich C. Drug delivery vehicles with improved encapsulation efficiency: taking advantage of specific drug carrier interactions. Expert Opin Drug Deliv. 2011;8(3):329-42. doi: 10.1517/17425247.2011.553216, PMID 21323506.
36. Wheatley AM, Kaduk JA, Gindhart AM, Blanton TN. Crystal structure of abiraterone acetate (Zytiga) C_{26} H_{33} NO_2. Powder Diffr. 2018;33(1):72. doi: 10.1017/S0885715618000015.
37. Blagden N, DE Matas M, Gavan PT, York P. Crystal engineering of active pharmaceutical ingredients to improve solubility and dissolution rates. Adv Drug Deliv Rev. 2007;59(7):617-30. doi: 10.1016/j.addr.2007.05.011, PMID 17597252.
38. Al Kassas R, Bansal M, Shaw J. Nanosizing techniques for improving bioavailability of drugs. J Control Release. 2017;260:202-12. doi: 10.1016/j.jconrel.2017.06.003, PMID 28603030.
39. Borba PA, Pinotti M, DE Campos CE, Pezzini BR, Stulzer HK. Sodium alginate as a potential carrier in solid dispersion formulations to enhance dissolution rate and apparent water solubility of BCS II drugs. Carbohydr Polym. 2016 Feb 10;137:350-9. doi: 10.1016/j.carbpol.2015.10.070, PMID 26686139.
40. Chang SH, Lin HT, WU GJ, Tsai GJ. pH Effects on solubility zeta potential and correlation between antibacterial activity and molecular weight of chitosan. Carbohydr Polym. 2015;134:74-81. doi: 10.1016/j.carbpol.2015.07.072, PMID 26428102.